Int. J. Nanosci. Nanotechnol., Vol. 12, No. 2, June 2016, pp. 119-130

Short Communication

The Effects of Different Seed Layers and Growth Time on the Quality of ZnO NRs Arrays

Z. Alaie[1], S. Mohammad Nejad[1], M. H. Yousefi[2] and S. Safarzadeh[1]

1. Nanoptronics research center, Iran University of Science and Technology, Tehran, Iran
2. Nanolab, Maleke Ashtar University of Technology, Shahin Shahr, Iran

(*) Corresponding author: alaie.zahra@yahoo.com
(Received: 23 January 2015 and Accepted: 21 February 2016)

Abstract

ZnO nanorods (NRs) were synthesized using an in situ low-temperature hydrothermal method. In order to investigate the effect of different seed layers on quality of ZnO NRs arrays, alcoholic, alkaline and acidic seed solutions were deposited by spin coating on ITO-glass substrate. Experimental results revealed that the vertically ZnO NRs obtained from monoethanolamine-based seed layer is the most uniform and compact one. Alkali solutions result in better alignment and uniform cross sections than those realized via acetic acid-based seed layer. Also, KOH- based seed layer show lower density and bigger cross section of ZnO NRs than that of NaOH based seed layer. Evolution of ZnO NRs layer was investigated by SEM images and UV-visible spectra at different growth times. By increasing growth time, the wavelength of UV-vis absorption edge exhibit a red-shift and the transmission of the light in visible and infrared regions decrease and therefore, the energy band gap of ZnO NRs decrease. Also, Oxygen plasma treatment resulted in increasing of UV absorption of ZnO NRs thin film. Scanning electron microscopy and X-ray diffraction spectra indicated that the crystalline ZnO NRs have rod shapes with hexagonal cross sections.

Keywords:*Hydrothermal synthesis, Thin film, UV photodetection, ZnO NRs.*

1. INRODUCTION

Since the discovery of ZnO NRs, they have been the target of numerous investigations due to their unique properties. These 1D structures reduced the carrier scattering because of quantum confinement in one direction. This improved the optical and electrical properties that enhance performance of devices based on ZnO thin film [1,2].

Wet chemical synthesis which is a low temperature, economical, facile manipulation, and scalable, have recently been developed for the production of vertically aligned ZnO nanostructures [3]. A considerable numbers of synthesis methods have been used to ZnO NRs fabrication, such as metal-organic chemical vapor deposition [4], metal-organic vapor phase epitaxy [5], thermal evaporation [6], vapor phase transport process [7] and thermal chemical vapor deposition [8]. But, these methods are complicated and need high growth temperatures. In comparison, the hydrothermal method [9, 10] is a simple, low temperature, high yield and more controllable process [11–14] than other mentioned methods. In this work, we report the hydrothermal growth of high quality ZnO NRs, which is a wet chemical method.

The fabrication procedure of hydrothermal method consists of two steps: (a) preparation of seed-layer and (b) growth of

NR arrays. This two-step approach allows the well- controlled growth of high quality, well-aligned ZnO nanoarrays with uniform morphologies [15].
Control of the orientation and morphology of ZnO nanostructures during the aqueous solution is difficult [16]. The ZnO seed layer plays an important role as nucleation sites in the growth of ZnO NR arrays and is essential to achieve well aligned NRs on the substrate. The ZnO seed layer with excellent crystal quality offers favorable surface for the aligned growth of ZnO NRs.
Previously, the effects of seed layers on the growth rate, diameter and density of ZnO NRs grown via aqueous solution routes have been investigated [17]. The different nucleation mechanisms in the VPT growth process of ZnO NRs on Si have been reported [18]. The effects of ZnO seed layer preparation conditions on the growth of ZnO NR arrays on a Si substrate have been investigated. ZnO seed films were prepared by different film deposition techniques such as thermal oxidation of metallic Zn film, direct current reactive magnetron sputtering deposition, radio frequency magnetron sputtering deposition and pulsed laser deposition [19, 20]. Also, a comparative study of ZnO NRs synthesized on monoethanolamine and KOH based seed layer using sol-gel method to fabricate ZnO NRs is reported. Although, the better crystal quality, fewer structural defect and better aligned ZnO NRs were obtained through monoethanolamine based sol-gel method, better electrical conductivity was obtained in ZnO NRs derived through KOH-based seed layer [21].
In this study we used different solutions for preparing ZnO seed layer on the ITO-glass substrate and the effects of seed layers on density and morphology of ZnO NRs were investigated. The morphology and optical properties of the ZnO NRs at different growth time have been reported.

2. EXPERIMENTAL

2.1. Effects of Different Seed Layers on the Density and Morphology of ZnO NRs Arrays

As mentioned before, the morphologies and crystallographic orientations of ZnO NRs are generally affected by the ZnO seeding layers, the NR growth was investigated using many different seed layers. In this work, For ZnO NR growth, different seed layers have been prepared using zinc acetate and different alcoholic, acidic and alkali solutions.
First, two coating solutions containing zinc acetate dehydrate (0.4 M and 0.7 M) with equivalent molar of monoethanolamine and 2-methoxyethanol ($CH_3OCH_2CH_2OH$, Merck, 99.5% purity) were dissolved. The resulting solutions were spun onto the substrate at the rate of 3000 rpm for 30 s at room temperature. Then the films were annealed at 500 ˚C for 30 min to remove the residual solvent. SEM images of films with these two concentrations are shown in Figure 1. Increase of Zinc acetate concentration results in formation of high density of ZnO NRs arrays, but the possibility of existence of impurities increases.

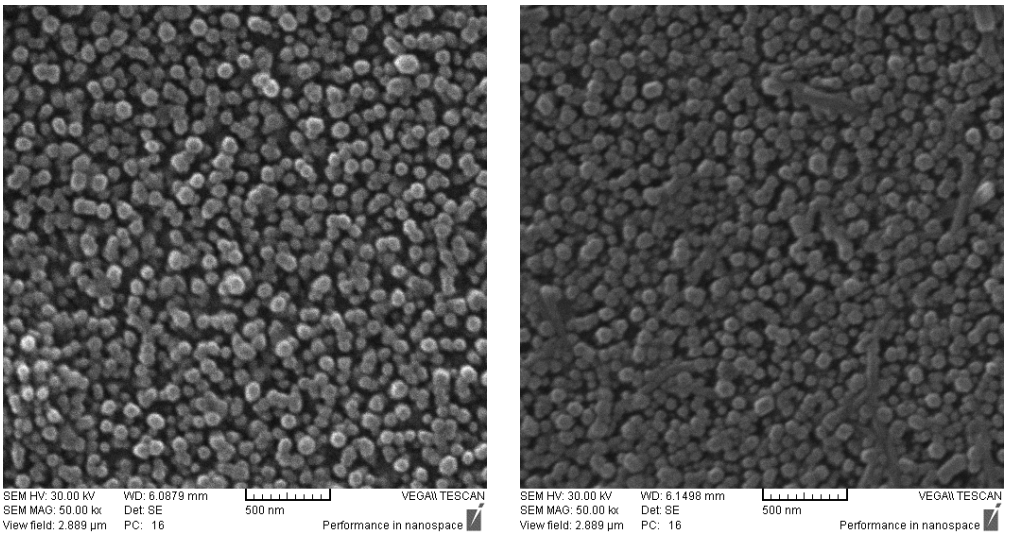

(a) (b)

Figure 1. *Top view SEM images of ZnO NRs were prepared by (a) 0.4 M and (b) 0.7 M seed solutions of the zinc acetate dehydrate, monoethanolamine and 2-methoxyethanol.*

In other methods, the seed layers were prepared by coating ZnO nanocrystal solutions. One solution was prepared by slowly adding an aqueous growth 30 mM of NaOH solution in methanol to a 10 mM zinc acetate dehydrate solution at 60 ˚C over a 2h period. The second nanocrystal solution was prepared by drop wise adding methanol solution of 30mM KOH in 10mM methanol solution of zinc acetate dehydrate at 60 ˚C. After 2 h of mixing, the solution was allowed to cool down. These two solutions show same PH (the molar concentration of hydrogen ions in the *solution*) about of 8. ZnO nanocrystals are obtained according to equation (1). The suspension of the nanoparticles (NPs) was spin coated on the ITO/glass substrates for 2 times at a speed of 3000 rpm. Thermal treatments were made to the substrates at 150 ˚C between each deposition.

Finally, a solution of zinc acetate (0.65 g) and acetic acid (a few droplets) in the 10 mL of anhydrous alcohol was spin-coated onto the ITO substrate. ZnO nanocrystals are obtained according to equation (2). Then, the films were sintered in air at about 150 ˚C for 30 min.

Figure 2 shows top view of ZnO NRs with seed layer deposited by KOH, NaOH and Acetic Acid solutions of zinc acetate dehydrate. Both of KOH and NaOH solutions result in ZnO NRs with uniformdensities and cross sections but because of larger atomic radius of potassium compared to sodium, ZnO NRs in figure 2a show lower density and bigger cross section than those in figure 2b. The seed layer of acetic acidic solution (figure 2c) results in ZnO NRs with different cross section and it yields considerable density of ZnO NRs.

$$Zn(CH_3COO)_2 + 2NaOH\,[2KOH] \rightarrow Zn(OH)_2 + 2CH_3COONa\,[2CH_3COOK]$$
$$Zn(OH)_2 \xrightarrow{temperature} ZnO + H_2O \quad (1)$$

$$Zn(CH_3COO)_2.2H_2O + CH_3COOH \Leftrightarrow CH_3COOH + Zn^{2+} + 2CH_3COO^- + 2OH^- + 2H^+$$
$$Zn^{2+} + 2CH_3COO^- + 2OH^- + 2H^+ \xrightarrow{temperatue} ZnO\downarrow + 2CH_3COOH\uparrow + H_2O\uparrow \quad (2)$$

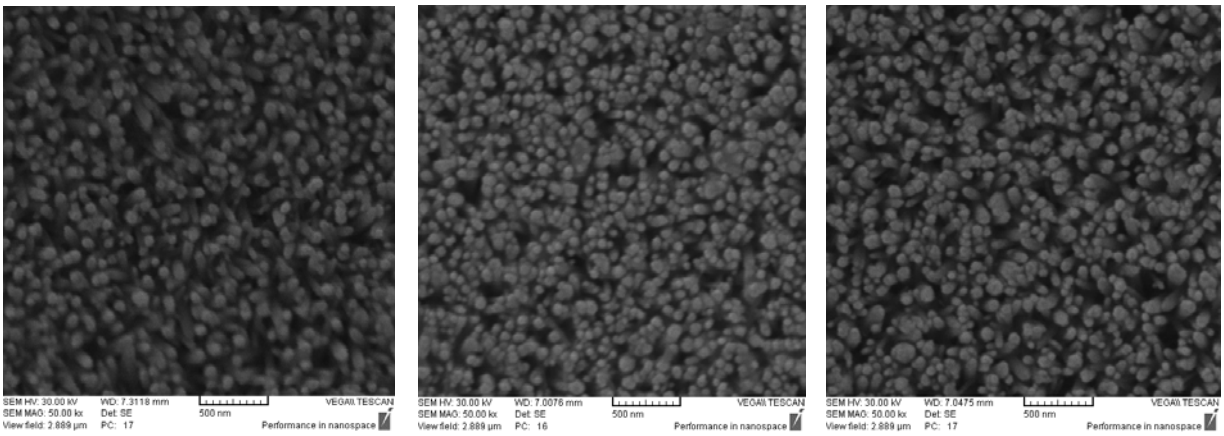

(a) (b) (c)

Figure 2. *Top view SEM images of ZnO NRs prepared by seed solutions of the zinc acetate dehydrate dissolved in (a) KOH, (b) NaOH and (c) Acetic Acid solutions.*

2.2. Growth of ZnO NR Arrays on ITO/glass Substrates

For hydrothermal synthesis of ZnO NRs, the seeded substrates were placed in 50ml of a 10mM $Zn(NO_3)_2 \cdot 6H_2O$ aqueous solution. Subsequently, 25 ml of 0.5M aqueous NaOH was added to the solution. Substrates with seed layers were immersed in the mixed solution with the seed layer side facing up. ZnO NRs have been synthesized according to equation (3):

$$\begin{aligned} &Zn(NO_3)_2 + 2NaOH \rightarrow Zn(OH)_2 + 2Na(NO_3) \\ &Zn(OH)_2 \xrightarrow{temperature} ZnO + H_2O \end{aligned} \quad (3)$$

To achieve better quality of the ZnO NR array, it is important to control the reaction rate. When temperature of reaction is too high, the reaction rate speeds up and the precursors consume rapidly, and nearly no ZnO NRs are found to stick on the ITO substrate in this case. For this reason, the glass bottle with the sample was then sealed and maintained at 70 ˚C for different times in order to grow ZnO NRs. After the reaction, the substrates were taken out and washed with deionized water several times to remove any residual salt or amino complex and then dried in air at room temperature. The main advantage of the proposed synthesis is its simplicity, low temperature (70 ˚C), and fast growth rates.

3. RESULTS ANDDISCUSSION

3.1. Morphology Evolution of ZnO NRs

We have investigated the morphology and optical evolution of the ZnO NR arrays with respect to different growth times. When the growth time (deposition time) increases, bigger and longer ZnO hexagonal NRs are obtained. In fact, the aspect ratio of the 1-D ZnO nanostructures depends on growth time. In order to illustrate the morphology evolution of ZnO NRs, a series of SEM images of prepared thin films in various stages during the growth are shown in Figure 3a-d.

ZnO NRs show whole hexagonal shapes, with different average diameters of 52.73, 78.12, 85.93 and 113.3 nm and lengths of 1.3 to 12.4 μm for 3, 6, 12 and 18 hr growth times, respectively. According to Figure 3a-d, through the deposition up to 6 h, the growth density is almost unchanged, and each ZnO NR has a constant diameter from the bottom to the top. After, with increasing growth time, densities of ZnO NR arrays decrease and NRs with different lengths and cross sections grow. Although crystal qualities of the ZnO samples get better with increasing the reaction time, because of low density of ZnO nanostructures, the alignment of ZnO NRs is low and they grow at different orientations (figure 3d).

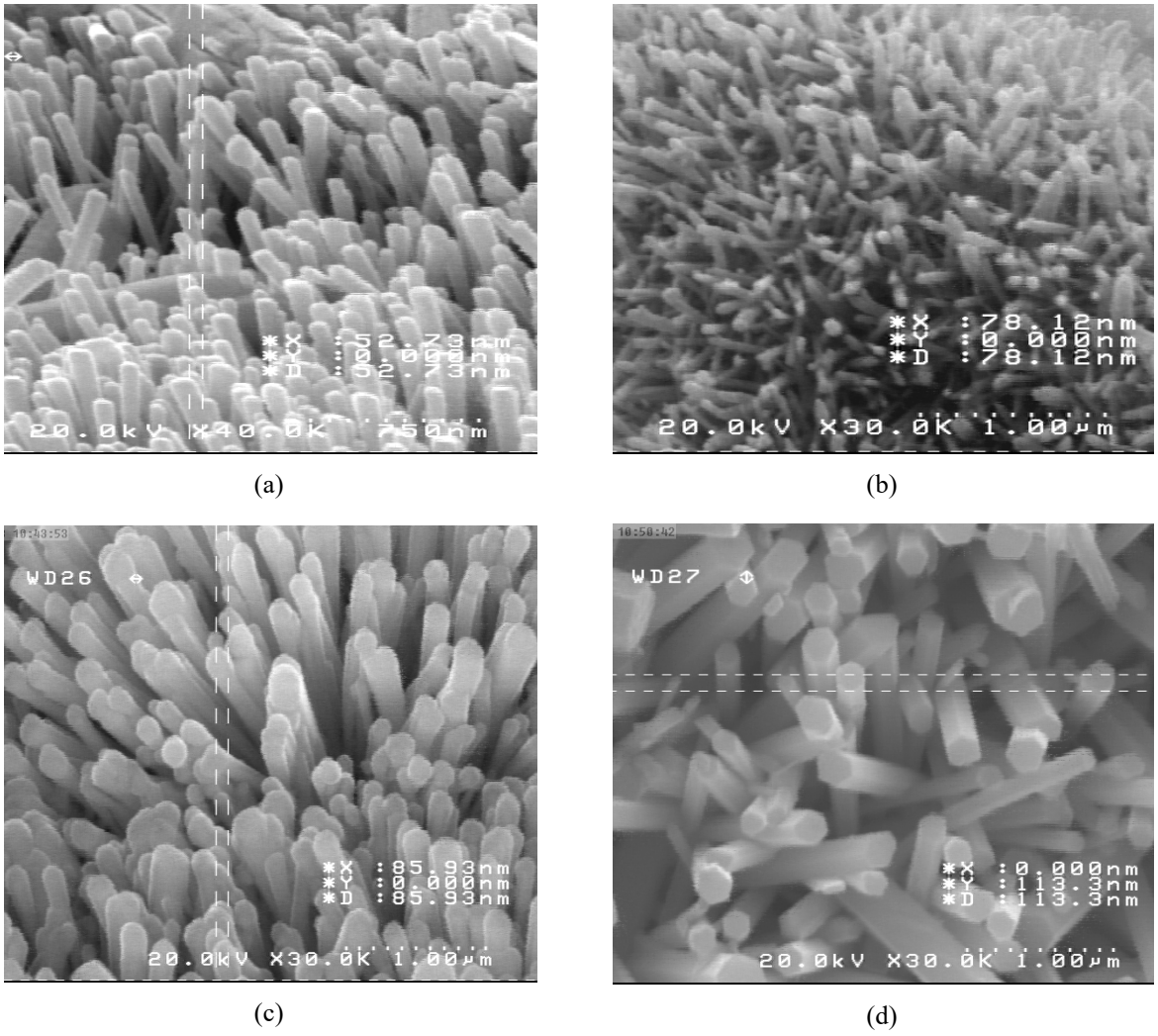

(a) (b)

(c) (d)

Figure 3. *ZnO NRs thin films obtained after (a) 3, (b) 6, (c) 12 and (d) 18 hr growth times.*

3.2. Optical Evolution of ZnO NRs

Also, UV-vis absorption spectra at different growth times were recorded for the investigation of optical evolution of the as-prepared products. ZnO NRs show blue shift enhanced UV-Visible absorption peak compared to ZnO bulk materials. Chen et al described blue-shift in UV-Visible spectra of ZnO NRs compared with that of ZnO materials spectra by size of ZnO NRs that was beyond the quantum confinement regime, which was ascribed to an enhanced surface effect due to a large surface-to-volume ratio [22].

In figure 4, the UV-Visible spectra of ZnO NRs after different growth time is shown. As you can see, the UV-vis absorption edge exhibits a red-shift by increasing the growth time. According to transmission spectra in figure 5, by increasing growth time, the transmission of the light in the visible and infrared regions decreases and absorption of the light increases.

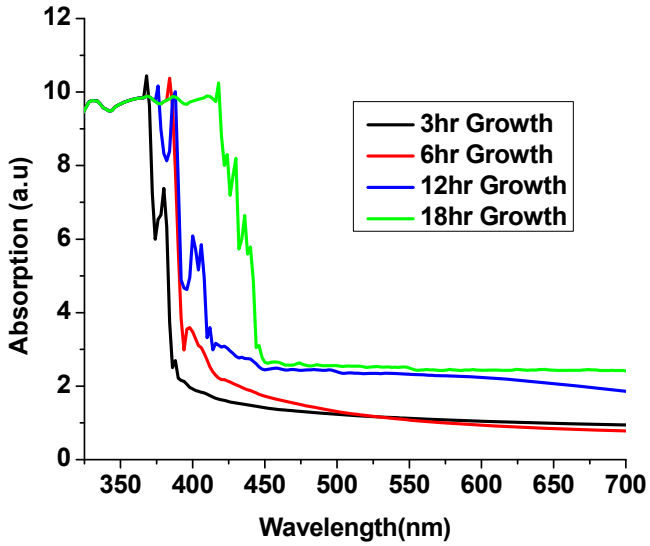

Figure 4. *UV-visible absorption spectra of ZnO NRs at different growth times.*

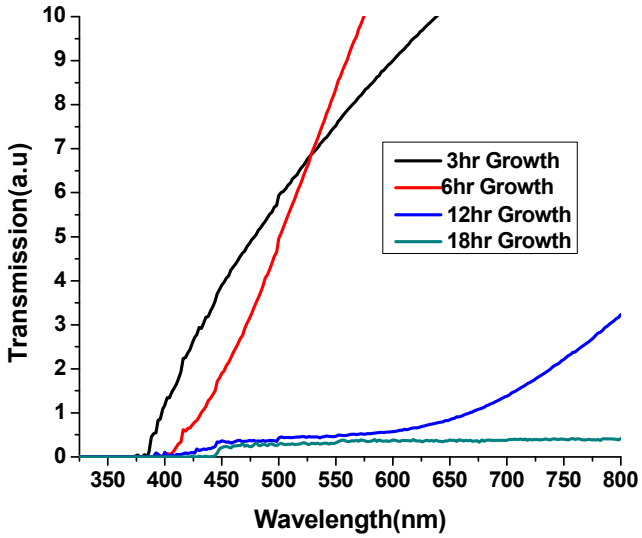

Figure 5. *Transmission spectra of ZnO NRs at different growth times.*

The low transmittance at the long growth time of the ZnO NRs suggests that the incident light is significantly blocked due to the strong scattering or reflection within the ZnO films or light absorption by ZnO rods with dimensions comparable to the wavelength of incident light. By using the data of the transmission spectra, the optical band gaps (*E*g) of ZnO can be estimated by using the conventional Tauc equation [23]:

$$\alpha h\nu = A(h\nu - E_g)^{n/2} \qquad (4)$$

Here α (α= -ln T) is the absorption coefficient, $h\nu$ is the photon energy and A is a constant. As a direct band gap semiconductor, the optical band gap (*E*g) of ZnO can be estimated by the zero crossing of the rising edge of the $(\alpha h\nu)^2$ vs $h\nu$ curve, as shown in Figure 6. For comparison, the estimated absorption edge wavelength (E_g), diameter and length of NRs obtained at 3, 6, 12 and 18 hr growth times are shown in table 1. By increasing the growth time, the size of ZnO NRs

increases and their energy band gaps decreases which gradually diverges from the intrinsic band gap of ZnO (3.37 eV). The band gap of ZnO NPs is in agreement with the theoretical calculation based on the effective mass model. The relationship between band gap and size of ZnO NPs can be obtained using effective mass model [24]. Using this model, the band gap E_g (eV) can be approximately written as:

$$E_g = E_g(bulk) + \frac{\hbar^2\pi^2}{2er^2}\left(\frac{1}{m_e}+\frac{1}{m_h}\right) - \frac{1.8e^2}{4\pi\epsilon_r\epsilon_0 r} \quad (5)$$

where E_g (bulk) is the bulk energy gap, r is the particle radius, m_e is the effective mass of the electrons, m_h is the effective mass of the holes, ϵ_r is the relative permittivity, ϵ_0 is the permittivity of free space, $\hbar$ is Planck's constant divided by 2π , and e is the charge of the electron. When *decreasing* the size of the *NPs* the energy states will become discrete, so that the energy *gap* will *decrease.* According to this model, by increasing diameter of ZnO NRs, band gap energy decreases that is consistent with our results.

The variation of energy band gap is affected by many factors. It is shown that the energy band gap of a ZnO thin film is affected by the residual strain, defect, and grain size confinement [25, 26, 27]. By increasing growth time of NR thin films, the average grain sizes enlarges from ~52 to ~113 nm and the film thicknesses increases from ~1.3 to ~12.4 nm, which result in the variation of strain. Prathap found the energy band gaps increased with the increase of film thickness and grain size in ZnS films fabricated by thermal evaporation [27]. Wang *et al.* also observed that the peak position of free excitonic emission red shifted from 3.3 to 3.2 eV with an increase of grain size from 21 to 64 nm, which was attributed to the quantum confinement effect [28].

In this work, the energy band gaps increasing with the increase of growth time might be related to the dependence of enhanced strain, enlarged grain size and more oxygen interstitials.

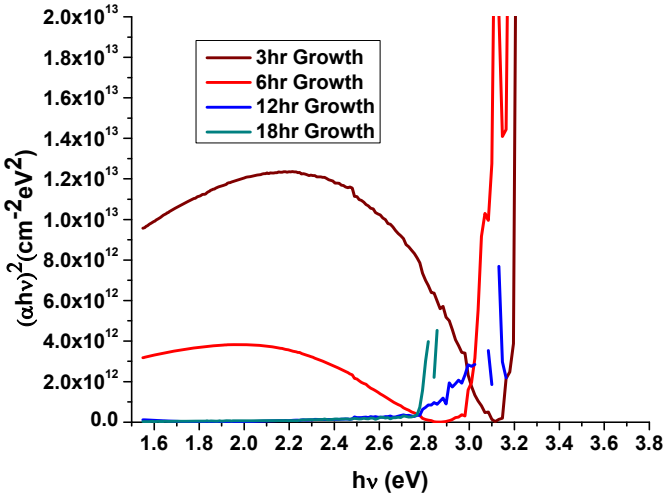

Figure 6. *(α hν)² vs hν curve of ZnO NRs at different growth times.*

Table 1. *Different estimated parameters of ZnO NRs at the different growth times.*

Growth time (hr)	Edge absorption wavelength (nm)	Band gap(eV)	Average diameter of cross sections (nm)	Length of ZnO NRs (μm)
3	368	3.12	52.73	1.3
6	390	2.9	78.12	-
12	400	2.78	85.93	-
18	435	2.72	113.3	12.4

Also, we have shown that oxygen plasma annealing increases UV absorption of ZnO (NRs) thin film. Figure 7 shows UV absorption before and after oxygen plasma treatment. The improved intensity of the UV absorption of the ZnO samples after plasma annealing indicates that the crystal quality of the ZnO samples gets better. Distinctly, the oxygen vacancies or structural defects in the ZnO samples decrease.

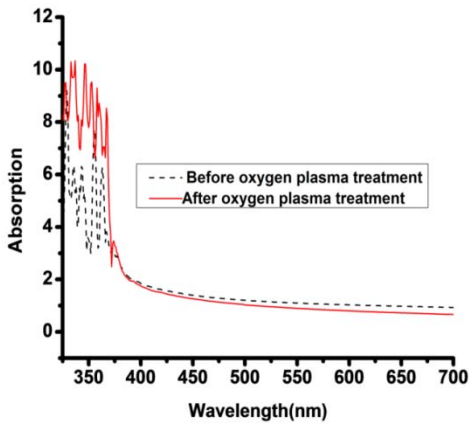

Figure 7. *UV absorption of ZnO NRs thin film before and after oxygen plasma annealing.*

3.3. X Ray Diffraction Results

The crystal phase and orientation of ZnO NRs were analyzed by X-ray diffraction. The XRD spectrum of ZnO NRs films fabricated at 70 °C for 3h is shown in Fig. 8. It is noteworthy to mention that the as-grown ZnO NRs are highly oriented along *c*-axis perpendicular to the substrate surface and only a single crystalline phase of ZnO is formed. Considering the growth direction of the ZnO NRs, the XRD result is fairly consistent with the hexagonal structure of ZnO (JCPDS: 75-1526) with lattice constants a = 3.22 A° and c = 5.2 A°. Also, no characteristic peak of any other impurities is observed in the spectrum.

The XRD pattern of the as-grown ZnO NR on glass substrate at 70°C and optimized deposition time of 3 hours has exhibited high (101) orientation indicating the preferential orientation of NRs.

A high single crystalline of ZnO NRs can provide direct electrical pathways to collect excited electrons. Thus, by controlling the surface to volume ratio and the growth orientation, the grown ZnONRs are quite suitable for photodetector fabrication with selective wavelengths.

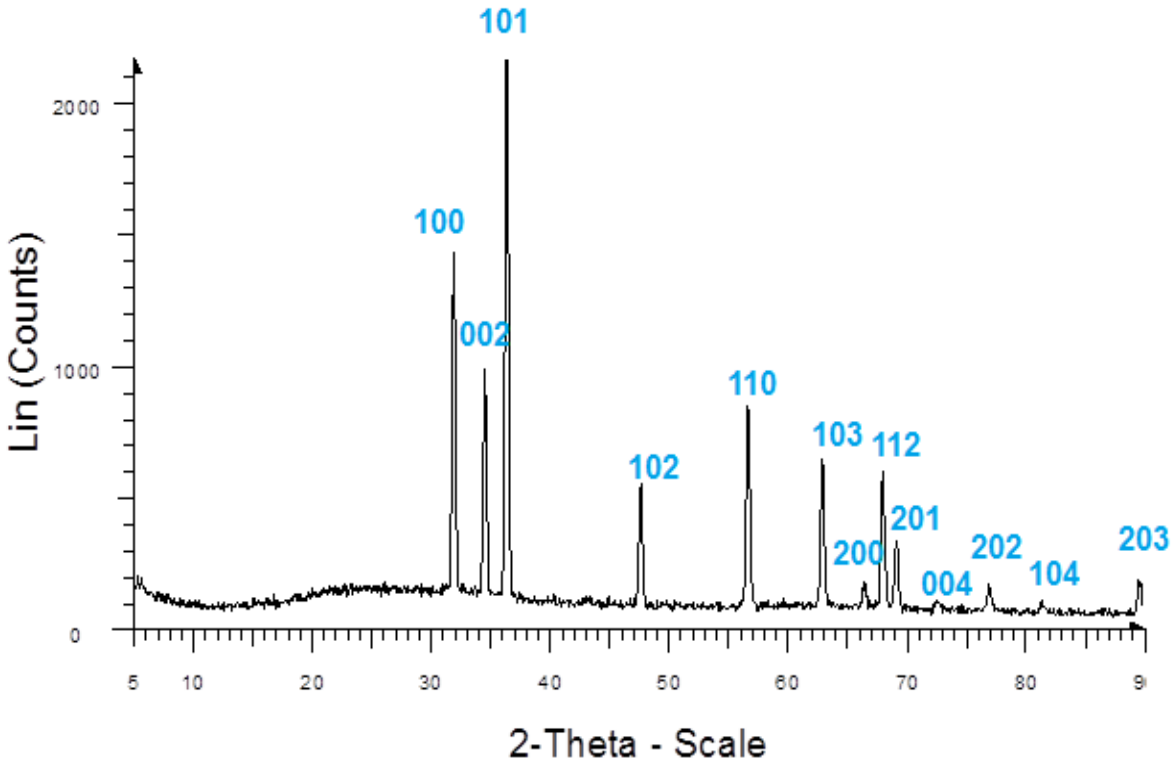

Figure 8.*X-ray diffraction spectrum of ZnO NRs. Coincidence of peaks with Lines of hexagonal structure is shown.*

3.4. Photoluminescence Analysis

Figure 9 shows the room-temperature Photoluminescence (PL) spectrum of the as-grown ZnO NRs arrays at room temperature. Experimental prepared ZnO NRs often show a sharp near-band-edge emission at 381 nm and a broad small visible light emission. The near band-edge emission is due to a well-known recombination of free excitons of the wide band-gap ZnO and the visible light emission is resulted from the recombination of photo-generated hole with a singly ionized charge state of specific defect. The narrow full-width at half-maximum (80 nm) of the PL spectra indicates the high crystal quality of the ZnO NR arrays. It is shown that the relative concentration of OH^-/Zn^{2+} regulates the luminescence properties of ZnO crystals as the green emission intensity decreases with an increase in OH^- concentration [29, 30]. In this synthesis, the ZnO NRs were prepared in a solution phase having a high pH (11.5), so that oxygen vacancy and therefore green emission in the ZnO NRs crystal was at a minimum.

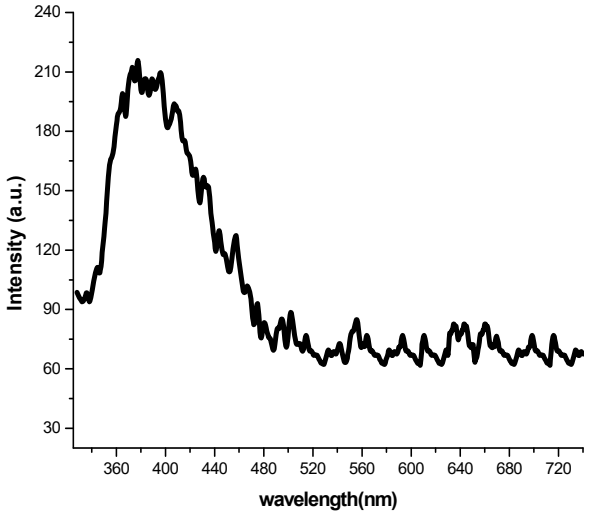

Figure 9. *PL spectrum of the ZnO NRs thin film at room temperature.*

4. CONCLUSION

In summary, we report the fabrication and characterization of the ZnO NR arrays on ITO-glass substrate by a two-step method. The effect of different seed layers on the morphology of ZnO NRs was investigated by SEM analysis. Higher concentration of zinc acetate and hydroxide alkali metals with small atomic radius as precursors in seed solution yield higher density of ZnO NRs. Seed layer made by alkali solution is more uniform than that by acidic solution. With increasing growth times, higher crystal quality, larger diameter, longer height, lower density and therefore lower alignment of vertically ZnO NRs were observed. Also, oxygen plasma treatment enhances UV absorption as a result of decreasing of oxygen defects. The spectrometric *luminescence spectra measurement*shows ZnO NRs with low impurities (green emission) as a result of suitable pH of growth solution and therefore good passivation of surface defects.

REFERENCES

1. Ma, X., Pan, J., Chen, P., Li, D., Zhang, H., Yang, Y., Yang, D. (2009). "Room temperature electrically pumped ultraviolet random lasing from ZnO nanorod arrays on Si", *Opt. Express*,17: 14426.
2. Lee, J. H., Ko, K. H., Park, B. O. (2003). "Electrical and optical properties of ZnO transparent conducting films by the sol–gel method", *Journal of Crystal Growth*, 247: 119-125.
3. Ahsanulhaq, Q., Umar, A., Hahn, Y. B. (2007)."Growth of aligned ZnO nanorods and nanopencils on ZnO/Si in aqueous solution: growth mechanism and structural and optical properties*",Nanotechnology*, 18: 115603.
4. Kim, K.-S., Kim, H.W. (2003). "Synthesis of ZnO nanorod on bare Si substrate using metal organic chemical vapor deposition"*, Phys. B: Condens. Matter*, 328(3): 368-371.
5. Ogata, K., Maejima, K., Fujita, S., Fujita, S. (2003). "Growth mode control of ZnO toward nanorod structures or high-quality layered structures by metal-organic vapor phase epitaxy", *J. Cryst. Growth,* 248: 25-30.
6. Wan, Q., Yu, K., Wang, T.H. (2003). "Low-field electron emission from tetrapod-like ZnO nanostructures synthesized by rapid evaporation", *Appl. Phys. Lett.*, 83: 2253-2255.

7. Grabowska, J., Nanda, K.K., McGlynn, K., Mosnier, J.P., Henry, M.O., Beaucamp, A., Meaney, A. (2005). "Synthesis and photoluminescence of ZnO nanowires/nanorods", *J. Mater. Sci.: Mater. Electron.*, 16: 397-401.
8. Wu, J. J., Liu, S. C. (2002). "Low-Temperature Growth of Well-Aligned ZnO Nanorods by Chemical Vapor Deposition", *Advanced Materials*, 14: 215-218.
9. Hirate, T., Kimpara, T., Nakamura, S., Satoh, T. (2007). "Control of diameter of ZnO nanorods grown by chemical vapor deposition with laser ablation of ZnO", *Superlattices Microstruct,*. 42: 409-414.
10. Xu, C.X., Wei, A., Sun, X.W., Dong, Z.L. (2006). "Aligned ZnO nanorods synthesized by a simple hydrothermal reaction", *Phys. D: Appl. Phys*, 39: 1690-1693.
11. Song, J., Baek, S., Lim, S. (2008). "Effect of hydrothermal reaction conditions on the optical properties of ZnO nanorods", *Phys. B: Condens. Matter*, 403: 1960-1963.
12. Vayssieres, L., Keis, K., S. Lindquist, A. Hagfeldt, (2001). "Purpose-Built Anisotropic Metal Oxide Material: 3D Highly Oriented Microrod Array of ZnO", *J. Phys. Chem. B*, 105: 3350-3352.
13. Liu, B., Zeng, C.H. (2003). "Hydrothermal Synthesis of ZnO Nanorods in the Diameter Regime of 50 nm", *J. Am. Chem. Soc.,* 125: 4430-4431.
14. Qiu, Z., Wong, K.S., Wu, M., Lin, W., Xu, H. (2004). "Microcavity lasing behavior of oriented hexagonal ZnO nanowhiskers grown by hydrothermal oxidation", *Appl. Phys. Lett.*, 84: 2739.
15. Ming-Yen, L., Ying-Jhe, W. (2015). "Selective growth of ZnO nanorods on hydrophobic Si nanorod arrays", *Nanotechnology*, 26: 055604.
16. Kar, J. P., Das, S. N., Lee, S. W., Ham, M. H., Choi, J. H., Myoung, J. M. (2009). "Surface modification of hydrothermally grown ZnO nanostructures with process parameters",*Chemical Engineering Communications*, 196: 1130-1138.
17. Song, J., Li, S. (2007). *"*Effect of Seed Layer on the Growth of ZnO Nanorods*", J. Phys. Chem. C,* 111: 596-600.
18. Zhao, D. X., Andreazza, C.; Andreazza, P., Ma, J., Liu, Y., Shen, D. (2005)."Buffer layer effect on ZnO nanorods growth alignment",*Chem. Phys. Lett.*, 408: 335-338.
19. Li, C., Fang, G. J., Fu, Q., Su, F. H., Li, G. H., Wu, X. G., Zhao, X. Z. (2006). "Effect of substrate temperature on the growth and photoluminescence properties of vertically aligned ZnO nanostructures", *J. Cryst. Growth*, 292: 19-25.
20. Li, Ch., Fang, G., Li, J., Ai, L., Dong, B., Zhao, X. (2008). "Effect of Seed Layer on Structural Properties of ZnO Nanorod Arrays Grown by Vapor-Phase Transport", *The Journal of Physical Chemistry C,* 112: 990-995.
21. Kashif, M., Hashim, U., Ali, M. E., Usman Ali, Syed M., Rusop, M., Ibupoto, Z. H., Willander, Magnus (2012). "Effect of Different Seed Solutions on the Morphology and Electrooptical Properties of ZnO Nanorods", *Journal of Nanomaterials*, 2012:452407, 6 pages.
22. Chen, Ch.-W., Chen, K.-H., Shen, Ch.-H., Ganguly, A., Chen, L.-Ch., Wu, J.-J., Wen H.-I., Pong, W.-F. (2006). "Anomalous blueshift in emission spectra of ZnO nanorods with sizes beyond quantum confinement regim*"*, *Applied Physics Letters*, 88: 241905.
23. Tauc, J., Menth, A. (1972). "States in the gap*"*, *Journal of Non-Crystalline Solids*, 8–10: 569-585.
24. Geng, B. Y., Wang, G. Z., Jiang, Z., Xie, T., Sun, S. H., Meng, G. W., Zhang, L. D. (2003).*"Synthesis and optical properties of S-doped ZnO nanowires"*, Applied Physics Letters, 82, 4791.
25. Mohamed, S. H., El-Rahman, A. M. A., Salem, A. M., Pichon, L., El-Hossary, F. M. (2006). "Effect of rf plasma nitriding time on electrical and optical properties of ZnO thin films", *Journal of Physics and Chemistry of Solids*, 67: 2351-2357.
26. Dong, B.-Zh., Fang, G.-J., Wang, J.-F., Guan, W.-J., Zhao, X.-Zh. (2007). *"*Effect of thickness on structural, electrical, and optical properties of ZnO: Al films deposited by pulsed laser deposition*"*, *Journal of Applied Physics*, 101: 033713.
27. Prathap, P., Revathi, N., Venkata Subbaiah, Y. P., Ramakrishna Redd, K. T. (2008). "Thickness effect on the microstructure, morphology and optoelectronic properties of ZnS films", *Journal of Physics: Condensed Matter*, 20: 035205, 10pp.
28. Wang, J., Gao, L. (2003). "Wet chemical synthesis of ultralong and straight single-crystalline ZnO nanowires and their excellent UV emission properties", *Journal of Materials Chemistry*,13: 2551-2554.
29. Kar, S., Dev, A., Chaudhuri, S. (2006). "Simple Solvothermal Route To Synthesize ZnO Nanosheets, Nanonails, and Well-Aligned Nanorod Arrays", *The Journal of Physical Chemistry B*, 110: 17848-17853.

30. Ghosh, R., Dutta, M., Basak, D. (2007). “Self-seeded growth and ultraviolet photoresponse properties of ZnO nanowire arrays”, *Applied Physics Letters*, 91: 073108.